We are IntechOpen, the world's leading publisher of Open Access books Built by scientists, for scientists

6,900
Open access books available

186,000
International authors and editors

200M
Downloads

Our authors are among the

154
Countries delivered to

TOP 1%
most cited scientists

12.2%
Contributors from top 500 universities

BOOK CITATION INDEX
CLARIVATE ANALYTICS
INDEXED

WEB OF SCIENCE™

Selection of our books indexed in the Book Citation Index
in Web of Science™ Core Collection (BKCI)

Interested in publishing with us?
Contact book.department@intechopen.com

Numbers displayed above are based on latest data collected.
For more information visit www.intechopen.com

Comparative Analysis of Bearings for Micro-GT: An Innovative Arrangement

Fabrizio Stefani, Andrea Perrone, Luca Ratto and
Ramon Francesconi

Additional information is available at the end of the chapter

Abstract

Microgas turbines are a widespread technology in cogenerative and propulsion applications. Bearings are a key factor in their design and development. The aim of the present research work is the development of the support system for a typical microturbine intended for power generation. To this goal, the present chapter defines the typical requirements of the machine and, afterward, describes the different technologies available to develop the support system of a reliable microturbine. Conventional (rolling element and oil-film) supports and cutting-edge (magnetic, aerodynamic, and aerostatic) bearings are reviewed. Particularly, their suitability to the operating conditions is compared by means of a literature review and elaboration of the relevant data. By analyzing all this information, a new concept for the design of a micro-GT support system is devised. Instead of using a single type of bearing as usual, the new system includes different types in order to take advantage of the best characteristics of each one and, simultaneously, to minimize the effects of the relevant flaws. The innovative support system requires a suitable bearing arrangement, which is compared with the conventional ones. The conceptual design of the innovation is completed by a discussion of its advantages, drawbacks, and prospective improvements.

Keywords: microturbine, gas-turbine, bearing arrangement, bearing performance, foil bearings

1. Introduction

Microturbine technology owes its origins to the military and aerospace industry, where the need of compact and high power density engines justifies significant production and development costs. Later, micro-gas turbine (micro-GT) units have been used in small-scale power

generation as well as cogeneration, and they are involved in the air compression as well as conditioning market. Recently, manufacturers are addressing their efforts to new market areas, for example, in powering hybrid electric vehicles as well as autonomous robots in the case of small-size machines.

In the following, such microturbines are intended as autonomous power generators. Despite their name, excluding portable devices and MEMS, typical shaft diameters of commercial microturbines are roughly 10 mm, and their electric power is in the order of 100 kW.

In the design of a microturbine, the bearing choice is not a trivial issue due to the high rotation speed and working temperature. In these operating conditions, the "classical" engine design criteria for choosing the most adequate bearing type (rolling or sliding bearings), which are based on dimensions and/or nominal power rate, cannot be adopted. According to such traditional design criteria, the choice for machines of small and large dimensions is unavoidable, i.e., rolling and sliding bearings are employed, respectively. For intermediate power machines, on the contrary, specific choices have to be carried out: on the one hand, rolling bearings have smaller overall dimensions and purchasing costs, and on the other hand, sliding bearings are more reliable.

Therefore, for microturbines, a comparative analysis of the available support systems, particularly focused on studying the influence of operating conditions (speed, temperature, and loads), is required. Accordingly, the present chapter provides a detailed comparison of bearing technologies by means of literature review and analysis of published data. Cutting-edge (e.g., magnetic, air, and ceramic bearings) and well-established solutions (e.g., steel rolling element and oil-lubricated slide bearings) are both considered in order to provide a large perspective.

On the basis of such a comparative study, an innovative design of a support system for micro-GTs capable of overcoming the limits of modern units is proposed. It employs different types of bearings and requires a proper design of their arrangement and coupling in order to take the maximum advantage of the peculiarity of each bearing. After a brief description of the existing bearing arrangements, the present chapter deals with the conceptual design of the new support system.

In synthesis, the present chapter defines the bearing requirements on the basis of design specifications of a typical micro-GT unit. Afterward, it studies the suitability of different bearing types for the operating condition requirements by means of a literature review. Finally, the innovative support system is proposed and compared with the current technical solutions.

2. Micro-GT design specifications

In a nutshell, the microturbines currently on the market have the design features described in the following references [1, 2]. They work according to a Brayton open cycle, which very often takes advantage of exhaust gases heat recuperation for air compressor discharge. The structure of these single-shaft microturbines includes an annular, or silo combustor, single-stage radial flow compressor as well as expander, and an optional recuperator. The electric power

ranges between 30 and 330 kW. They work with low pressure ratios (typically in the range 3–5), high nominal rotation speeds (ranging between 43,000 and 116,000 rpm), and relatively low efficiency (17–20% for simple cycle machines and around 30% for recuperated machines). The design life is usually between 60,000 and 80,000 hours with overhaul [3]. Turbine entry temperatures range between 700 and 1000°C, while exhaust temperatures are in the range of 260–310°C (for recuperated machines).

Accordingly, **Table 1** reports the main data of a micro-GT unit designed in a previous work [4], which can be assumed as the typical machine and reference for subsequent calculations.

Design variable (unit)	Value
Rotational speed N (rpm)	70,000
Shaft diameter D (mm)	15
Electric power P (kW)	110
Pressure ratio	4
Inner radius of compressor blades (mm)	7.5
Outer radius of compressor blades (mm)	59
Inner radius of turbine blades (mm)	7.5
Outer radius of turbine blades (mm)	72.5
Turbine torque M_t (N m)	30
Compressor torque M_c (N m)	−15

Table 1. Main data for the design of the reference micro-GT unit.

2.1. Bearing external loads

Table 2 gathers the bearing loads computed for the reference unit. The total radial load is due to the shaft weight, and it is directed downward. The positive direction of the axial forces listed in **Table 2** is from compressor to turbine, as also shown by the direction of *z*-axis in **Figure 1**.

The total thrust load is computed as the algebraic sum of compressor and turbine axial forces. Both of the forces are the resultant of the axial thrusts exerted on the blades and on the backside of the impellers by the working fluid.

Consequently, together with the area of the impeller backside, the pressure on the clearances between casing cover and impeller back shroud (backside pressure) plays an important role in determining the nominal axial thrusts, which are plotted in **Figure 1** as a function of the backside pressure. By means of CFD simulations, a backside pressure equal to 0.25 MPa (Case A) has been calculated so that both the impeller thrusts are directed toward the external side of the unit. Nevertheless, for different impeller geometries, which may yield different pressure drops between compressor delivery and clearances, compressor, turbine, and total thrust directions can reverse, as shown by **Figure 1**, for backside pressures lower than 0.15 MPa, and as a conse-

quence, such cases (both thrusts directed toward the inner side of the machine) must be taken into account. To this purpose, for the same reference value of the total axial load (500 N) Case B is identified in **Figure 1**. The axial loads in both Case A and B are summarized in **Table 2**. An axial force reversal can also occur during transient operation, e.g., the start/stop phase of the unit.

Design variable (unit)		Value
Radial load (rotor weight) W (N)		40
Total thrust load (absolute value) T_{ref} (N)		500
Axial thrust on compressor blades (N)		2100
Axial thrust on turbine blades (N)		−3010
Case A	Pressure on the back side of the impellers (gauge) (Pa)	250,000
	Compressor thrust T_c (N)	−600
	Turbine thrust T_t (N)	1100
Case B	Pressure on the back side of the impellers (gauge) (Pa)	80,000
	Compressor thrust T_c (N)	1200
	Turbine thrust T_t (N)	−1700

Table 2. Loads acting on the bearings of the reference micro-GT unit.
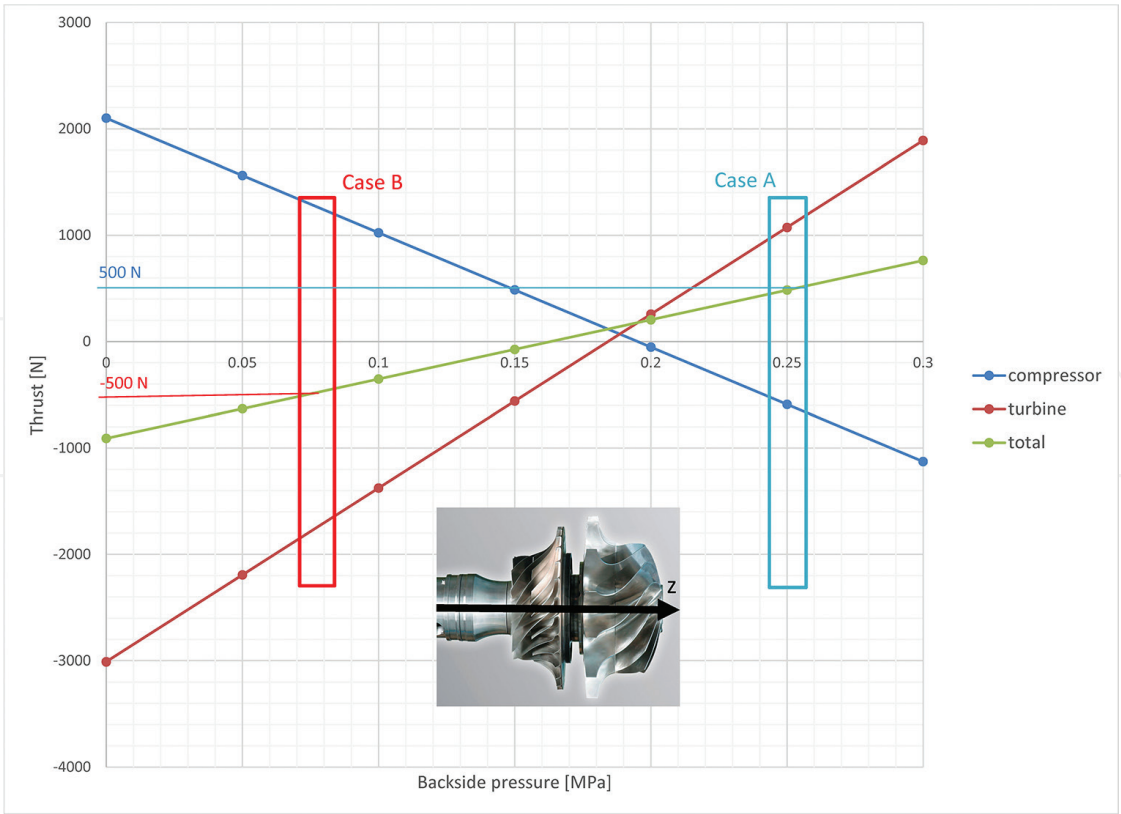
Figure 1. Compressor, turbine, and total thrust acting on the shaft in nominal conditions for the reference micro-GT as a function of the backside pressure.

2.2. Bearing requirements

Requirements are related to the operating conditions of the units (operative speeds and temperatures) and bearing performance (duration, load-carrying capacity, and power loss).

The high rotation speeds of micro-GT shafts yield different problems (e.g., ball spinning, centrifugal loading, and skidding), which have greater effect on larger bearings. Therefore, an important requirement is that bearings have a high peripheral speed limit.

In the following, the effect of peripheral velocity is quantified in terms of the DN speed factor (where D is the diameter of the shaft housing expressed in mm, and N is the rotation speed expressed in rpm).

Micro-GT units must usually operate in high-speed conditions, which for rotors are usually characterized by speed factors ranging between 1×10^6 and 2×10^6 mm rpm. In ultra-high-speed rotor applications DN overcomes 2×10^6 mm rpm, as in the case of mobile power systems [5], which are beyond the scope of the present paper.

Indeed, in the case of the reference microturbine, the operative speed factor is roughly 1×10^6 mm rpm (see **Table 1**) so that bearings with DN limit lower than such operative value must be discarded.

In addition, the bearings must operate throughout the domain of possible temperature conditions of the microturbine. Such temperatures range between 100 and 1000°C in nominal operation, while during start-up, they extend down to room temperature. Expected working temperature of the bearings depends on their location and relevant thermal management, e.g., type of cooling or vent.

Bearing duration should preferably overcome 70,000 hours (the average duration of the units) and should not be limited by the number of start/stop cycles so that maintenance and bearing replacements could be minimized.

Reasonably, predicted axial load is a magnitude order higher than radial load (**Table 1**). The former load is significant as far as metal fatigue and wear are concerned, while the latter is so light that it may cause stability problem at high speed in self-acting radial bearings.

Since the state-of-the-art efficiency of microturbines is quite low, bearings must not reduce further this value. To this goal, they should be designed for the minimum power loss (e.g., friction) and their possible power input should not be significant.

Finally, depending on the shaft layout, resonance eigenfrequencies usually occur at a speed lower than the operating one; therefore, the vibration amplitude should be limited by the bearing damping.

3. Bearing comparison

The adequacy of the most reliable types of bearings is studied. To this purpose, the behavior of the following types of bearings is analyzed:

(1) steel rolling element bearings, lubricated by grease or oil;

(2) sliding bearings, lubricated by oil;

(3) air (film) bearings;

(4) magnetic bearings;

(5) ceramic bearings.

The first two categories include conventional bearings, taken as a reference for performance comparison. The last item includes rolling element bearings entirely manufactured in ceramic material and hybrid bearings, made up of steel rings and ceramic balls, with or without film coatings on the races.

Only supports based on well-established technology are analyzed, while research solutions (still in development), such as squeeze film bearings, hydroinertia gas bearings, ferrofluid bearings, and metal mesh foil bearings, are not considered.

The assessment of compliance of the different bearing types with micro-GT operating conditions, including speed (DN factor), temperature, and loads, requires a proper comparison of literature and technical data.

3.1. Operating speed

Operative and absolute speed limits of the different bearing solutions are compared in **Figure 2**.
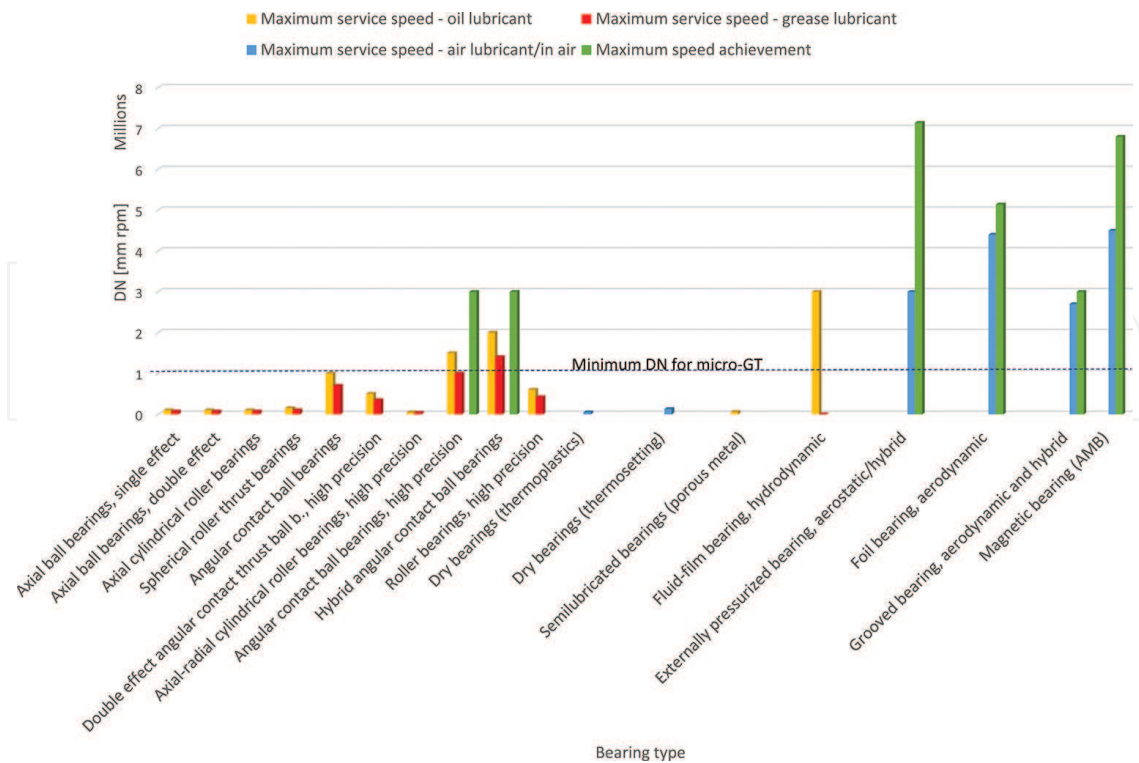
Figure 2. Maximum speed factors for different bearings.

The speed limit of rolling element bearings is mainly due to the skidding of the elements on the rings [5]. Among such bearings, high-precision angular contact ball bearings by means of suitable tolerances, osculation, rolling element size, and number can reach the high speed required by micro-GT (DN > 1 × 10⁶ mm rpm). The maximum DN reached by high-precision ball bearings is about 3 million mm rpm [6, 7]. Higher DN values can be reached by angular contact bearings by means of specific lubrication systems [8].

Manufacturer's catalogs (SKF, Schaeffler) show that the use of ceramic balls in place of steel ones can yield an operating speed increase of roughly 20–30%. Such a result is confirmed by the data reported in reference [9], i.e., speed of hybrid bearings can be increased by 20–30% compared with conventional ones. Accordingly, in comparison with steel bearings, a 60% decrease of centrifugal load matched with the 30% load capacity reduction predicted by Hertz theory finally provides a maximum allowable increase in rotation speed of just 32%. It decreases to 10% for all ceramic bearings.

The DN operative limit reported for oil-lubricated slide bearings regards bearings of turbines for power generation plants [10] and for induction motors [11]. In such cases, operative speed is only restricted by strength limits and by the allowable temperature. In microturbine applications, the operative speed of slide bearings is also limited by their stability and suitable bearing geometries are required, e.g., elliptical and pocket bearings, multilobe bearings, tilting pad bearings (listed from least to most stable).

Waumans et al. [12, 13] report that the highest achieved DN-number for a self-acting bearing operated in air is 7.2 × 10⁶ mm rpm. It is reached by an aerodynamic journal bearing stabilized by means of a grooved bush with a wave-shaped geometry as well as a flexible and damped support structure.

As far as foil bearings are concerned, maximum speed is relevant to a Ø8 mm bearing for microturbines operating up to 642,000 rpm (DN = 5,136,000 mm rpm) from results in reference [14].

Among the grooved bearings, the maximum operative DN of a Herringbone grooved journal bearing (HGJB) with enhanced grooved geometry [15] is 2.7 × 10⁶ mm rpm, and it is lower than foil bearing one. In addition, experimental results confirm that grooved hybrid bearings (GHBs) can run satisfactory at speeds in excess of 3.0 × 10⁶ rpm mm. Nevertheless, such DN is assumed as upper speed limit for grooved bearings, as they are prone to destructive whirl instability at ultrahigh speed [16].

Hybrid aerostatic bearings are suitable due to both the aerostatic stabilizing effect at high speeds and the low air consumption, which has extremely small effect on the global efficiency [17]. For a proper operation, they require air supply at high speed, when it is actually available in micro-GT systems. Data relevant to the maximum speed reached by aerostatic bearings refer to reference [18]. The relevant maximum operative speed is also documented in reference [19].

In today's industrial applications, active magnetic bearing (AMB) rotational speeds are in the range of about 180,000 rpm for a grinding spindle, or about 300,000 rpm for small

turbo-machinery [20]. The latter value, by assuming D = 15 mm as suggested by **Table 1**, corresponds to DN = 4.5 × 10⁶ mm rpm, which is confirmed by the data suggested by SKF. Anyway, by means of carbon fiber bandages in the rotor, 6.8 × 10⁶ mm rpm can be reached [19]. Such a value is a documented maximum speed for actual applications rather than a maximum theoretical limit, which is unknown as in the case of air foil bearings [21].

3.2. Operating temperature

Table 3 lists the maximum operational temperatures of the bearings.

Bearing type	Max operating temperature (°C)
Rolling element	125–315
Ceramic hybrid	350
Ceramic integral	800
Oil sleeve (journal)	125–150
Oil tilting pad	125–150
Hydrostatic	125–150
Magnetic (AMB)	500–600
Magnetic (PMB)	150–300
Aerodynamic, air foil	650
Aerodynamic, rigid/grooved	500
Aerostatic	900

Table 3. Maximum operating temperatures for different bearing types.

As far as steel rolling bearings are concerned, in addition to the lubrication system and the lubricant characteristic, steel reaction to heat and dimensional stability influences their endurance at high temperature. Generally, hardness of steel starts to decrease as temperature rises over 200°C. In addition, as steel heats up, phase transformation occurs and the bearing parts expand. The maximum dimensionally stable temperature ranges between 120 and 250°C, depending on steel type (source: NSK). Accordingly, a limit temperature of 180–260°C for rolling element bearings is indicated in reference [21]. Similarly, a 125–150°C operative limit for AISI 52100 bearings that can be specially stabilized up to 200°C and up to 315°C by using tool steel bearing materials is reported in reference [10]. The authors of reference [11] confirm that operative temperature is usually kept below 150°C except for heat-stabilized bearings.

Ceramic bearings behave better than steel rolling bearings at high temperature. Indeed, hardness and strength of silicon nitride do not deteriorate at high temperatures when compared with those of bearing steel. Particularly, the advantage of all ceramic bearings over hybrid

bearings consists especially on the major capability of working in dry or underlubricated conditions, at high temperature (<800°C) and corrosive environment [9]. Such a suitability to high temperatures is confirmed in reference [10], which indicates a limit of 650°C for ceramic bearings with vapor phase lubrication or solid lubricants.

Hydrodynamic bearings are the most limited in operating temperature. Indeed, such a limit comes from bearing surface and oil endurance. Soft metal and Babbitt limit upper temperatures are usually in the 125–150°C range [10]. Limit operating temperature of hydrocarbon oils is 93°C [22], while high temperature oils can also reach 150–200°C, e.g., silicon oils. Therefore, oil lubricated slide bearings are ultimately limited in temperature by bearing surface resistance.

Gases can be employed as lubricants over an extremely wide range of temperatures. For gas bearings, operating temperature limits come from shortcomings of solid components (journal and bearing material), not of the lubricant. Electric motors with ceramic windings supported by gas bearings can work for long periods at temperature up to 500°C [23], which is assumed as the limit temperature for aerodynamic bearings.

Foil bearings require the use of a solid lubrication to prevent wear and reduce friction during instances of contact, i.e., at low-speed conditions at start-up and shutdown. Since common lubricants, e.g., graphite and moly-disulfide (MoS_2), are limited to 150°C, solid lubrication is often obtained on the shaft and top foil layer by means of thin, soft polymeric film and sacrificial coatings. Innovative coatings, e.g., nanocomposite for journals and CuAl alloy for top foils, can reach temperatures as high as 650°C, which not by chance is also the limit operating temperature indicated for foil bearings in reference [21]. By using well-established tribo-solutions like polymer coatings, air bearing operation is roughly limited below 300°C [24].

Ceramic aerostatic bearings can reach a temperature as high as 800°C [23] and, in general, temperatures up to 900°C and speeds up to 65,000 rpm are feasible for externally pressurized gas bearings [25]. Indeed, aerostatic bearings have the highest temperature limit among the bearing analyzed. It is higher than temperature limit of aerodynamic bearings due to the external air supply, since air cools as it expands. In addition, the very low friction losses avoid thermal expansion due to viscous heating.

Among magnetic bearings, a great drawback of passive magnetic bearings (PMBs) comes from high temperature operation requirements of micro-GT systems, as permanent magnet stability is affected by temperature. Maximum practical operating and Curie (demagnetization) temperatures for the major classes of permanent magnet materials are in the ranges of 150–540 and 310–860°C, respectively. On the contrary, AMBs can work in extreme temperature environments (500–600°C) [21].

3.3. Load-carrying capacity and life

The maximum specific loads for the bearing types in analysis are summarized in **Table 4**.

Bearing type	Max service-specific load (MPa)
Rolling element	2
Ceramic hybrid	2
Ceramic integral	2
Oil sleeve	2.1
Oil tilting pad	4.4
Hydrostatic	6
Magnetic (AMB)	0.8
Magnetic (PMB)	0.4
Aerodynamic, air foil	0.7
Aerodynamic, rigid/grooved	0.1–0.2
Aerostatic	0.2

Table 4. Maximum service-specific loads for different bearing types.

For rolling element bearings, the "carrying capacity" is the ability of the bearing to carry a given load for a predetermined number of cycles or revolutions [26].

The maximum documented specific load for rolling element bearings operating in gas turbines is reported in reference [21]. **Table 5** reports the durations of bearings in a shaft support system designed by means of catalog high-precision rolling bearings solely. They are computed according to the adjusted basic rating life [27] by using data in **Table 1** and radial as well as thrust loads in **Table 2**. It is assumed that radial load is equally distributed between two sets of high-precision angular contact bearings and only one (locating) set carries the axial load in order to allow the thermal dilatation of the shaft. The solutions with both 2 and 5 matched bearings in the sets (in tandem arrangement) that carry the axial load are not satisfactory compared with the machine life (about 70,000 hours).

Set	L_1 (h)	L_{10} (h)	L_{50} (h)
One bearing, radial load W	267,960	1,276,000	6,380,200
Two bearings, radial load W and axial load T_{ref}	65	310	1549
Five bearings, radial load W and axial load T_{ref}	451	2150	10,747

Table 5. Expected life for sets of angular contact high-precision bearings, carrying half of the rotor weight and, if specified, the axial load.

Dynamic load ratings of steel bearings can also be used for ceramic bearings of the same dimensions [28], since from test results and predicted values service life of ceramic bearings is longer than that of steel bearings, except for heavy loads.

For the remaining bearings, fatigue is not the main concern, and the external load can be treated as static.

Sleeve bearings life is theoretically infinite and extremely long when they are properly maintained. Significant wear may occur only during extended start-up or coast-down periods, as mixed lubrication occurs at low speed. If the frequency of such events is high, hydrostatic jacking is recommended to minimize bearing wear [11].

Load capacity of oil-film bearings is basically a function of speed and oil viscosity so that high temperature plays a role by reducing viscosity. Many specifications limit motor bearing specific pressures to 1.4 MPa, which is often compliant with structural strength. Nevertheless, most journal bearings safely tolerate pressures beyond 2 MPa, as reported in reference [10]. Tilting pad thrust bearings for turbines carry further increase of specific load, and pads are subject to elastic deformation.

Generally, as hydrodynamic and hydrostatic bearings distribute the load over a larger area than rolling element bearings, their load capacity can be higher. Particularly, hydrostatic bearings can support huge loads, higher than hydrodynamic supports, as their pressure distribution is more uniform.

Air (aerostatic and foil) bearings, because of the different film layer, approximately support only a fraction of the load carried by hydraulic bearings with the same dimension. Indeed, specific load capacity of air foil bearings is 0.7 MPa [21], which is roughly one-fifth of the specific load for hydrodynamic bearings (3.5 MPa, on average). Differently, specific load for aerostatic bearings is lower due to a further constraint. Indeed, aerostatic bearings are typically limited to operate at less than 10 atm of pressure (usually 0.69 MPa) for safety reasons and due to the lubricant compressibility, which yields much higher flow rates and pumping power demand for the same pressure in comparison with liquid lubricants [29]. Such value is much lower than supply pressure of hydrostatic bearings, which typically operate at 20–40 atm but can reach 200 atm, when space is not limited and large loads must be supported. Specific load capacity (load per pad area) for aerostatic and hydrostatic bearings is the efficiency multiplied by supply pressure, where the efficiency is typically 25–40%.

According to the basic rating life formula [27], for constant duration load-carrying capacity of rolling element bearings drops as speed rises. On the contrary, load capacity of foil bearings is proportional to rotational speed. Hence, foil bearings outperform rolling element bearings at high speeds [30] but require solid lubrication at low speed in order to reduce friction and wear. Particularly, conventional solid lubrication systems, i.e, thin polymer films, enable over 100,000 h of operation before requiring a major overhaul. Beyond the temperature limits of polymer coatings (300°C), innovative coatings (PS304, Korolon) have demonstrated lives in excess of 100,000 h start-stop cycles under moderate loads (0.34 MPa) and high temperatures (ranging between 178 and 650°C) where such solid lubricants become active. However, bearing operating life is cut by over half (roughly 33,000 cycles) at room temperature (25°C), where the coating does not perform as well [24]. For low temperature start-ups, usually under higher loads, life may further decrease [31].

In order to characterize the behavior of foil bearings by means of a suitable map, in reference [32], a modified Sommerfeld number S' is correlated with the specific power loss. Foil journal bearings must be designed so that they operate in the high speed (or lightly loaded) regime

(S′ > 6) of the operating map plotted in **Figure 3** in agreement with the suitable regression proposed by the reference authors. Particularly, the nominal working point should be located in the high-speed (lightly loaded) regime, but significantly far from the shaft strength and thermal limits (specific power loss lower than 155,000 W/m²).
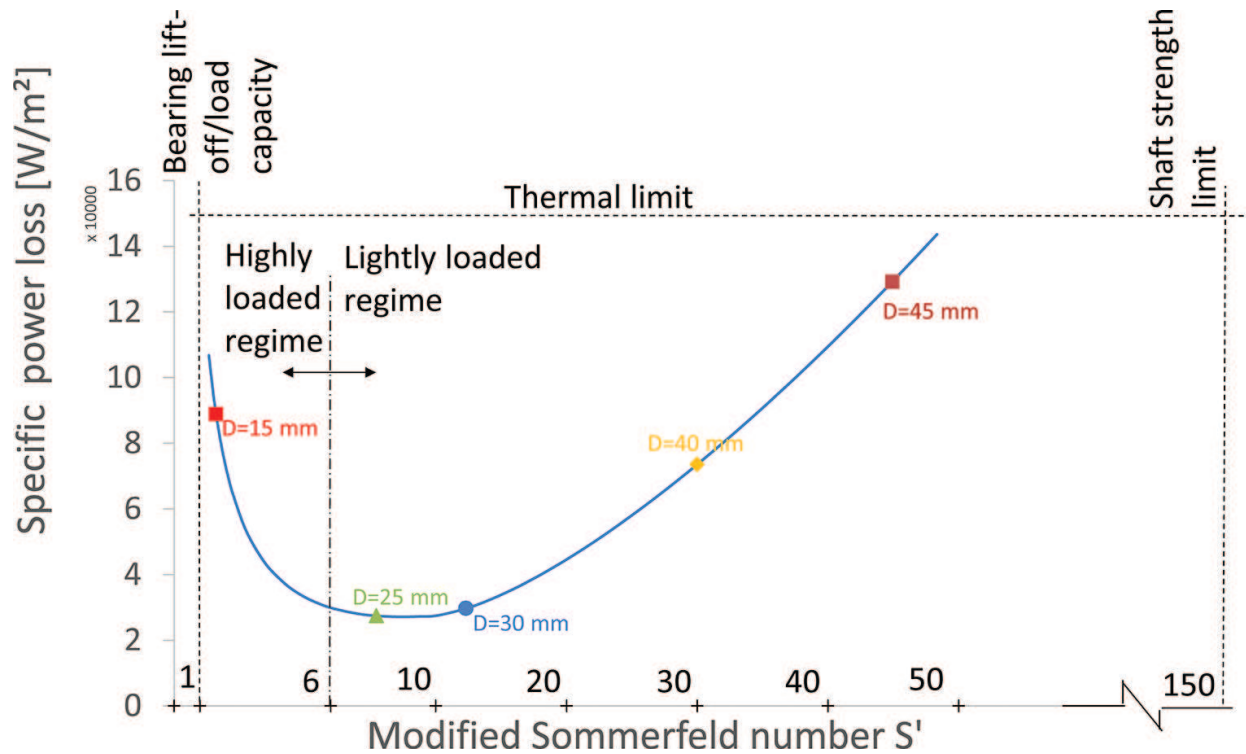
Figure 3. Performance map of foil bearings and operating points of the reference micro-GT for different journal diameters.

In order to locate in the operating map the nominal working point of a single radial foil bearing supporting the reference microturbine shaft, the data reported in **Table 1** are used together with unit (axial) length to diameter ratio (L/D = 1), load coefficient equal to 2.7×10^{-4} N/(mm³ krpm) (third-generation bearings) and isoviscous behavior assumption. In addition, the total load is approximated by the external one (40 N) as first estimate. By means of such assumptions, the assessment of S′ according to reference [32] suggests that the working conditions are not suitable (S′ = 1.6 < 6). Therefore, the journal diameter must be increased (optimal values range between 25 and 40 mm, as suggested in **Figure 3**). Indeed, transitioning over to oil-free lubrication requires suitable design solutions in that thin shafts are not required anymore to avoid rolling element bearings from operating above their DN threshold. On the contrary, large diameter hollow shafts must be used in order to increase the peripheral speed and, as a consequence, the load capacity of air bearings [31].

As far as the remaining air film bearings are concerned, the different fluid film bearing designs (multilobe and tilting-pad geometries) achieve better stability than plain bearings at the expense of load-carrying capacity. On the contrary, gas-lubricated grooved bearings promise stability with minor reduction of lift [33].

Magnetic bearings have advantageous load-carrying characteristics, whereas load does not drop as speed decreases. Nevertheless, if the electromagnets are unable to support the applied load because they are undersized or malfunctioning, the shaft cannot be levitated and the machine shuts down [34]; therefore, backup bearings are required to protect the rotor against overloads and power loss.

Reasonable specific loads for AMBs range between 0.3 and 1 MPa. Particularly, the maximum specific load value reported in **Table 4** is suggested for AMBs in reference [21] on the basis of the data published in references [35, 36].

For a stacked structure of PMB fabricated using neodymium-iron-boron magnets with a remanence of 1.3 Tesla (42 MGOe magnetic field), the maximum specific load, referred to the axial cross section (LD), is roughly 0.4 MPa and the corresponding axial specific load is 0.6 MPa [37].

Life expectancy of passive bearings is very high, i.e., in excess of 20 years. As AMBs include more components (controllers, coils, and sensors) and a laminated rotor, their life is expected to be shorter but, anyway, AMBs can still last 20–30 years with proper substitutions of failed components.

4. Innovative support system

The conclusion of the review study is that each bearing type has different strengths and weaknesses. Therefore, by using different types of bearings in the same support system, a proper design of their arrangement should be capable of taking the maximum advantage of the peculiarity of each bearing.
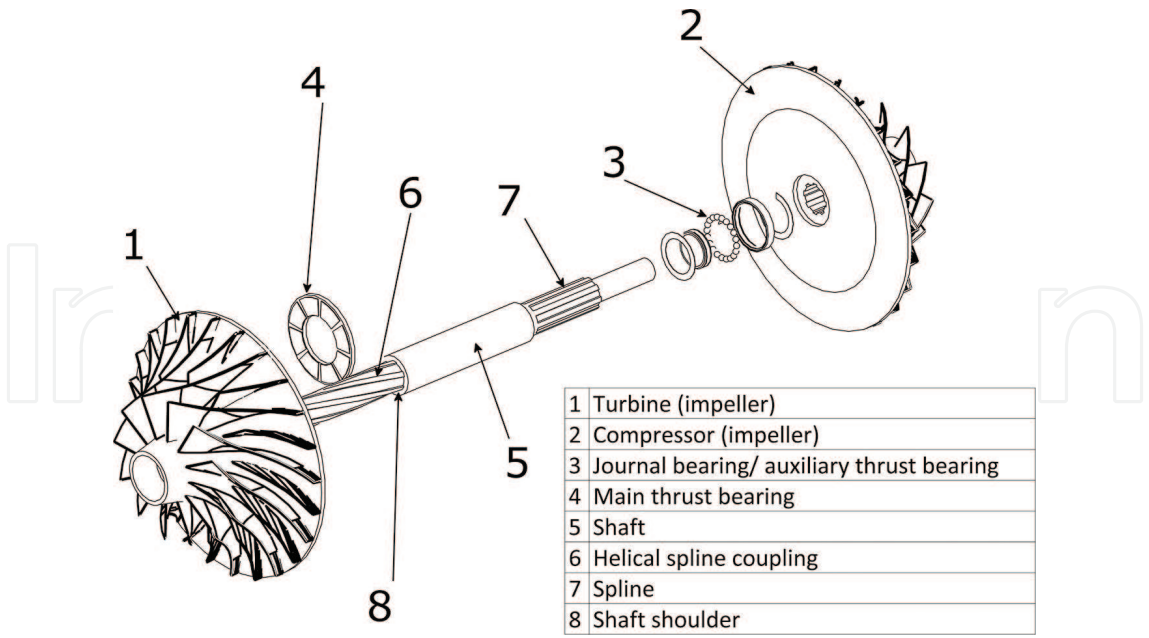
To this end, the conceptual design of an innovative support system, which takes advantage of both foil and rolling element bearings, is presented.
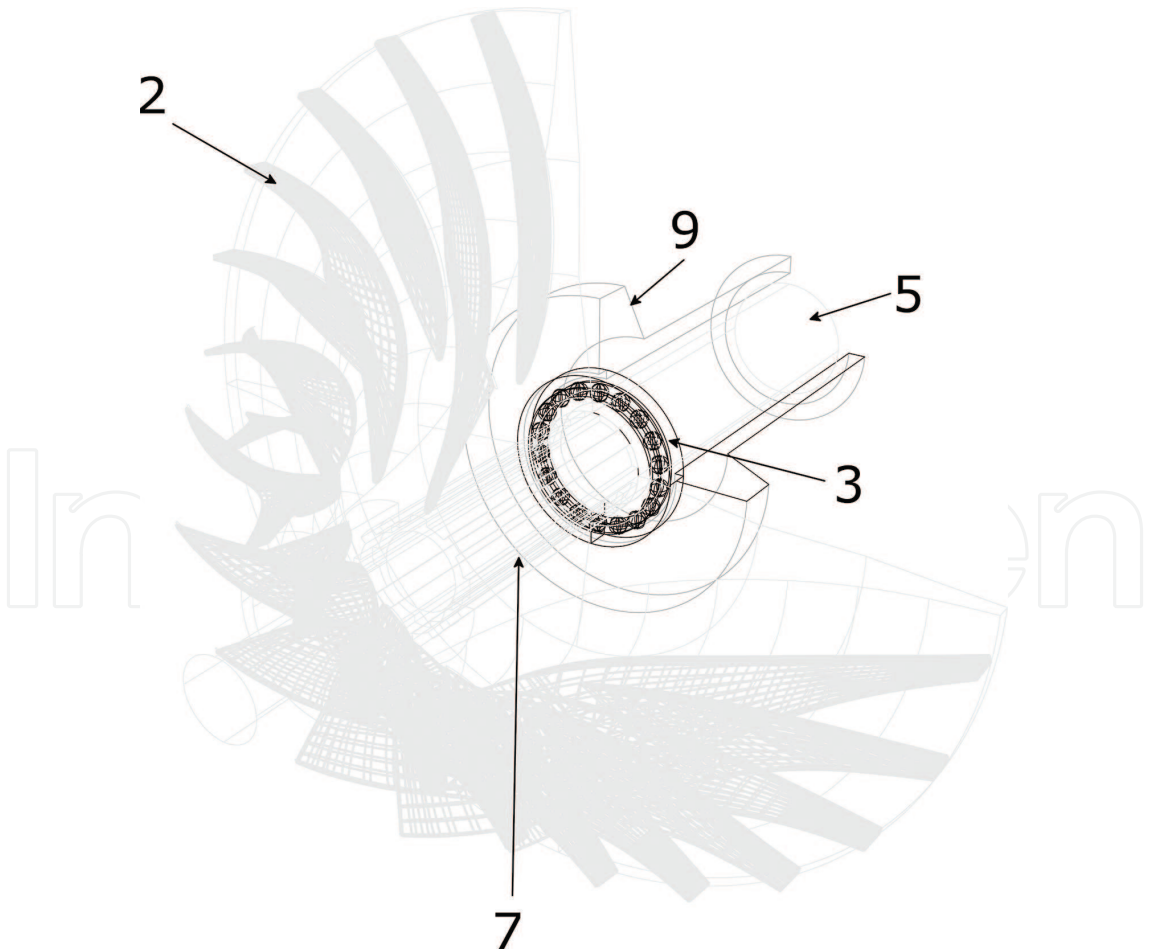
4.1. Layout and components

A simplified scheme of the assembly of the cutting-edge support system is depicted in **Figure 4**. In the simplified scheme of the invention used, hereafter load direction is assumed as in the Case B of **Table 2**.

The angular contact ball bearing (3), at the compressor side (**Figure 4**), is capable of carrying both radial and axial loads. As axial load may reverse during start-up of the unit, the bearing must have double effect, i.e., it is made up of two (or more) matched single-row bearings in back-to-back arrangement. Although four-point contact ball bearings are normally not available for precision (high speed) applications, a single bearing is depicted in **Figure 4** for the sake of conciseness of the scheme and clarity. As shown in **Figure 5**, such a bearing is mounted by inserting the external ring inside a suitable bore on the machine frame (9) and by placing the inner ring onto the relevant seat on the shaft with proper tolerances. Particularly, the outer ring must be axially constrained in order to carry thrust loads (locating bearing).

| 1	Turbine (impeller)
2	Compressor (impeller)
3	Journal bearing/ auxiliary thrust bearing
4	Main thrust bearing
5	Shaft
6	Helical spline coupling
7	Spline
8	Shaft shoulder

Figure 4. Simplified assembly of the innovative support system.

Figure 5. Ball bearing seat and spline coupling at compressor side.

A possible second radial support (always of rolling element type, e.g., a set of angular contact ball bearings in back-to-back arrangement) has not been included in **Figure 4** for simplicity. Nevertheless, it would be useful to avoid that the shaft is in a cantilever configuration, and it should be able to carry radial load solely. Therefore, such additional radial bearing should not be constrained axially to the housing on the frame (nonlocating bearing) so that the axial thermal expansion of the shaft would be allowed.

The plate of the foil bearing, i.e., component (4) listed in **Figure 4**, is fixed to the frame as shown in **Figure 6**, where the runner surface is located on the back of the turbine rotor (1) and the opposite sliding pairs, runner (11) and pads (12), are separated by the clearance c_z. A suitable spacer (10) must allow a proper adjustment of the clearance (or preload in static conditions) to ensure optimal operation of the foil bearing.
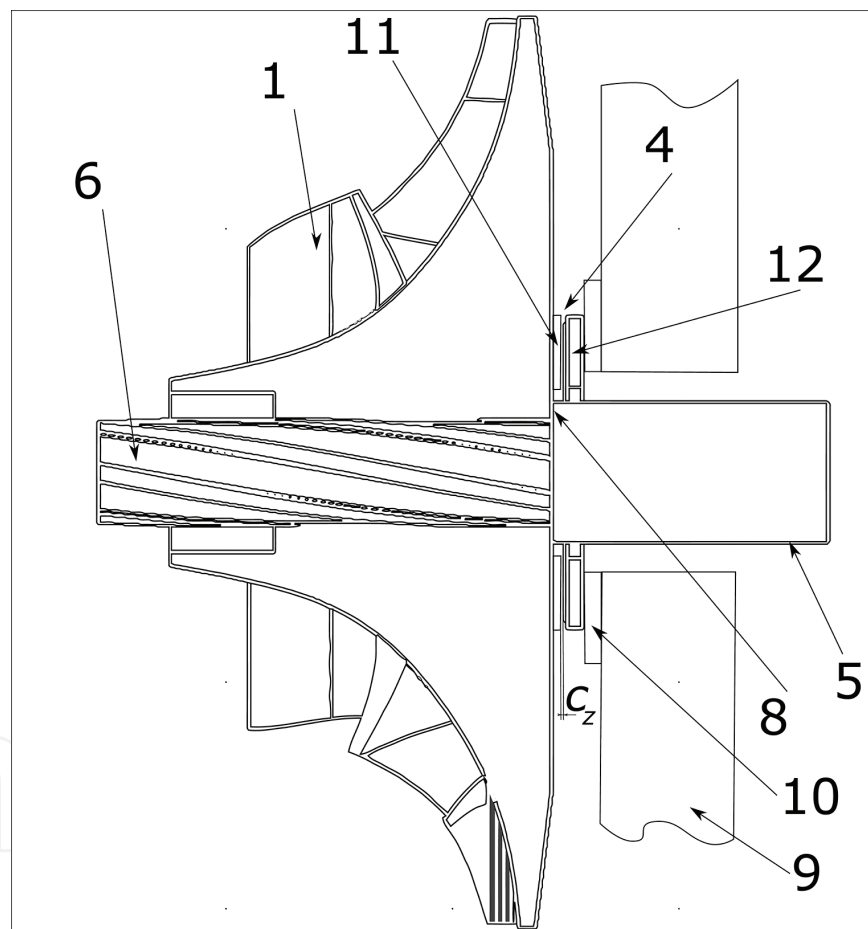
Figure 6. Foil air bearing installation and adjustment.

When the foil bearing has no aerodynamic load-carrying capacity, the turbine thrust acts on the shaft shoulder (8). Differently, after an air film is formed and the relevant aerodynamic pressure is generated, its micrometric thickness causes the runner/impeller assembly (1) to move accordingly in the axial direction so that the contact between the turbine impeller hub and the shaft shoulder does not occur anymore. Consequently, in nominal conditions and

starting from the rotation speed at which the runner is airborne, the only axial load transfer from the turbine to the shaft may occur through the helical spline coupling, as a function of the design helical angle.

Figure 4 also illustrates the coupling between the impeller hubs and the shaft (5). The compressor impeller (2) is fixed by means of a conventional spline pair (7) (made up by equally spaced straight grooves), the profile of which is depicted with parallel sides (or straight teeth). Differently, on the turbine side, a helical spline pair (6) (in which each groove forms a helix around the shaft) is machined. Such particular spline fit provides the additional function of axial load distributor. Of course, involute instead of parallel-side profiles may be chosen for both compressor and turbine wheel spline pairs. The purpose of the helical spline pair is to distribute the axial load between main (4) and auxiliary (3) thrust bearings, as explained in the following paragraphs.

4.2. Main thrust bearing relief

The innovative layout and, particularly, the direct matching of turbine impeller and main thrust bearing (4) allow for its relief during start/stop of the unit.

With reference to thrust loads and symbols given in **Table 2** (Case B), let $F_t = -T_t$ and $F_c = T_c$ be the turbine and compressor thrusts, respectively (**Figure 7**). They are caused by the pressure of the evolving fluid on the relevant impellers.
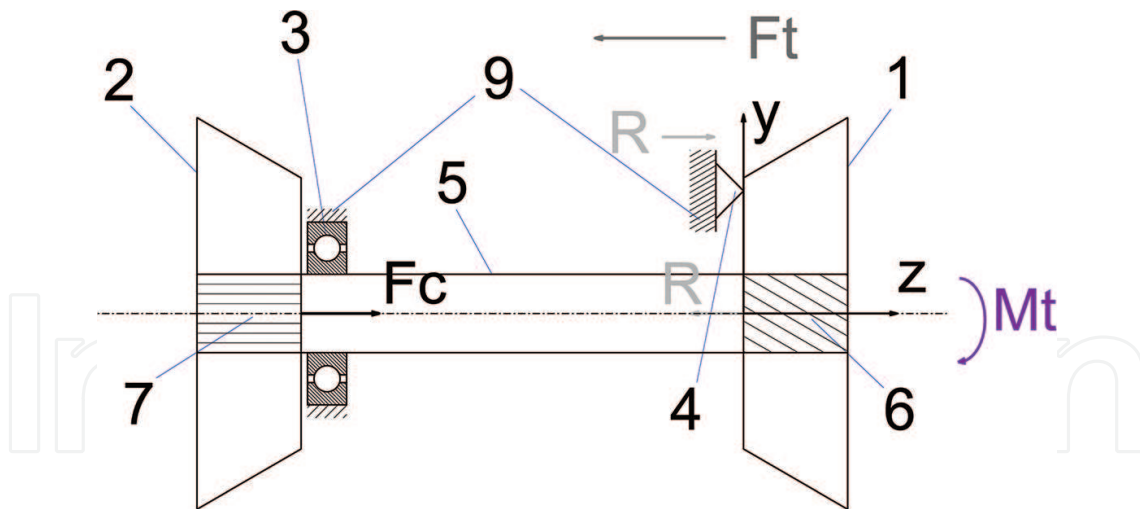

Figure 7. Static scheme (axial forces) of the innovative rotor operating in nominal conditions.

At start-up and until the onset of the aerodynamic lift, the auxiliary bearing (3) carries the whole thrust so that the main thrust bearing (4) is unloaded, and therefore, it works with minimal or no wear. Indeed, in such a condition, the turbine impeller (1) exerts the thrust F_t on the shaft shoulder (8) (visible in **Figures 4** and **6**) instead of on the foil bearing (4). Through the shoulder and the shaft, the thrust F_t is then transferred to the shaft support, i.e., the auxiliary bearing (3), like in a conventional bearing layout. Once the runner of the main bearing becomes

airborne at sufficient speed and a consequent translation of the turbine impeller occurs, auto-matically it relieves the auxiliary one, as the shaft shoulder (8) does not receive thrust anymore.

4.3. Load partition

According to the explanation of the previous paragraph, in nominal working conditions with no helical spline fit (e.g., by adopting a straight grooved spline on turbine-side too), the whole thrust of the turbine F_t would be carried by the main thrust bearing and the compressor thrust F_c would be supported by the auxiliary bearing. In a conventional shaft-bearing assembly, the reference thrust T_{ref} that loads the single axial bearing comes from the opposite thrusts exerted by turbine and compressor, i.e., $T_{ref} = F_t - F_c$. Therefore, during nominal operation in compari-son with a conventional support system, the new assembly design would disadvantage the main thrust bearings, whereas $F_t > T_{ref}$. Differently, by taking advantage of the (turbine-side) helical spline pair as an actuator, a part of the turbine thrust can be transferred from the hub to the shaft. In such a way, any wanted division of the thrust load between the two (main (4) and auxiliary (3)) bearings can be obtained as a function of a single design parameter, i.e., the spline helix angle β shown in **Figure 8**.
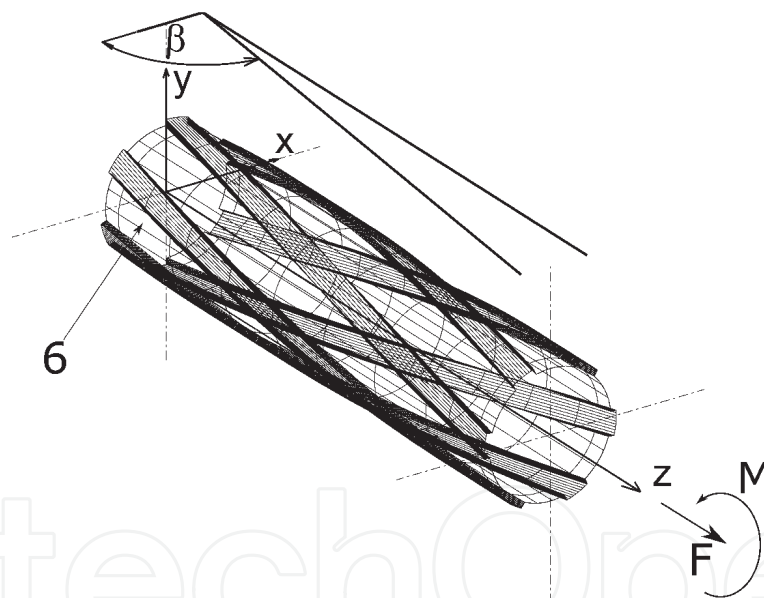
Figure 8. Helix angle and reference system of spline coupling.

Particularly, by means of a suitable choice of the helix angle in the design phase, in nominal conditions, it is also possible to subject the main axial bearing to a thrust T_{ref} as in a conven-tional support system, while the auxiliary bearing remains axially unloaded. In such a case, as this support is an angular contact ball bearing, it carries solely the radial load, the intensity of which is much lower than the axial loads. Obviously, this is only an example of load divi-sion. The new layout allows us the setting of the optimal load division in the design phase as a function of the load-carrying characteristics of the bearings, as well as expected duration and reliability of rolling element supports.

4.4. Law of load distribution

First, the law of load distribution followed during nominal operation by the helical spline pair, employed as a mechanical actuator besides a simple coupling system, is determined.

Figure 7 depicts the forces acting in nominal conditions on the rotor components according to the modifications resulting from the innovation. The constraint simulates the main axial bearing (4), which carries the load F_t–R. The axial forces R are the (equal) action and reaction that the turbine impeller exerts on the shaft through the helical spline. The total thrust that acts on the shaft is F_c–R and is carried by the auxiliary axial bearing (3). The torque M_t is the resisting torque of the turbine due to the pressure exerted on the relevant blades.

A campaign of FEM structural analyses has been carried out on a model of helical spline coupling (**Figure 9**) with parallel-side profiles by varying the design helix angle β from 45 to 135°. Reference system and helix angle β of the spline coupling model are shown in **Figure 8**. In agreement with the helix angle definition, the middle of the range (β = 90°) corresponds to a spline with rectilinear generatrices (straight teeth).

As shown in **Figure 9**, the spline and hub submodels are merged into the coupling model by means of contact elements. Two load cases are analyzed, where the hub section of one model end is submitted to either the axial load F_t or the torque M_t according to the values in **Tables 1** and **2**. Suitable constraints are added to the other end of the model, i.e, zero displacement components d_r, d_θ, and d_z in cylindrical coordinates.
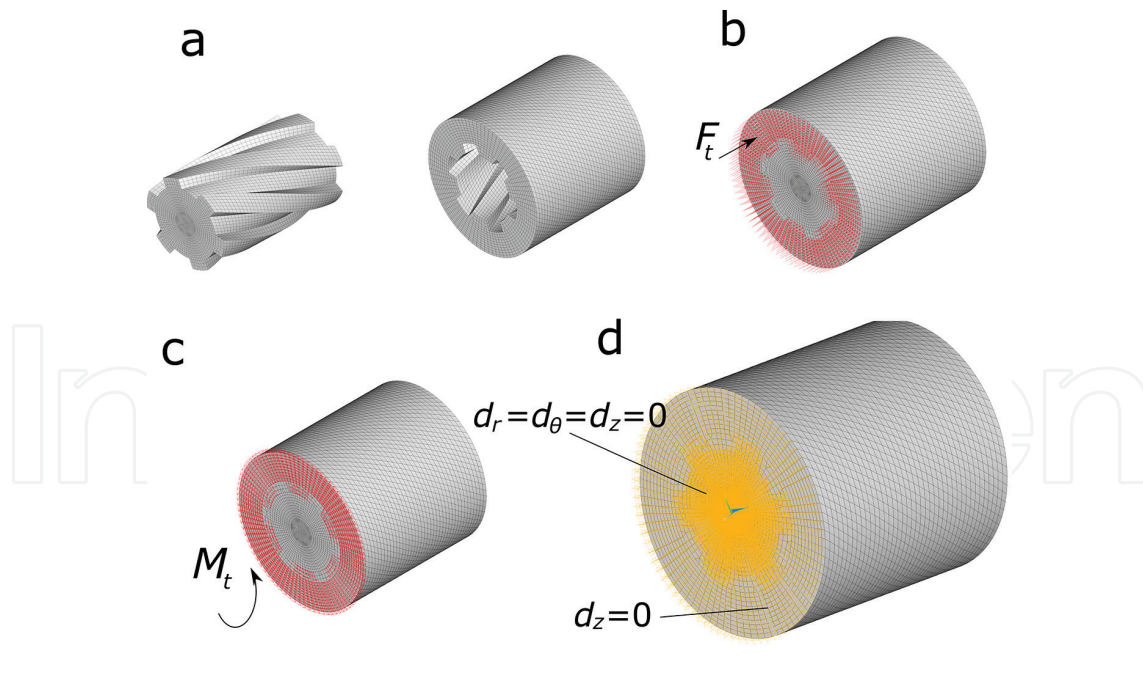
Figure 9. FEM model of helical spline coupling (β = 70°): (a) mesh of shaft and hub, (b) axial force loading, (c) torque loading, (d) boundary conditions.

Numerical results evidence that statics of spline couplings obeys two important rules. First, the load transfer through the spline due to the axial thrust F_t is small (6.7% of the thrust for β = 135° deg, i.e. the helical angle of maximum load transfer), and it is caused by deformations

of the kinematic pair. In other words, if the hub and the shaft were perfectly stiff, the turbine thrust would not be transmitted at all to the shaft through the spline surfaces, but it would be carried by the constraint (4), i.e., the main axial bearing. Second, the load transfer R from the hub to the shaft through the spline due to the torque M_t is actually ruled by the following relationship, valid for a spline pair with perfectly stiff members

$$R = \frac{M_t}{r_p \tan\beta} \tag{1}$$

where r_p is either the pitch radius in case of involute splines or the inner radius for parallel key splines.

Figure 10 compares the shaft and hub reactions computed by means of Eq. (1) and the FEM model with frictionless contact elements (torque load case). The shaft thrust is the reaction that the constraints exert on the grooved part of the shaft, and it represents the load transfer R from the hub to the remaining part of the shaft through the spline surfaces. The hub thrust is equal and opposite according to Newton's third law. Therefore, in case of compliant members, the rule defined by Eq. (1) is still valid with negligible error (0.6% of the transmitted load for β = 135°). Equivalently, the compliance of the kinematic pair members does not yield perceivable effects for the nominal value of torque M_t. Details of the FEM analyses will be published in the near future.
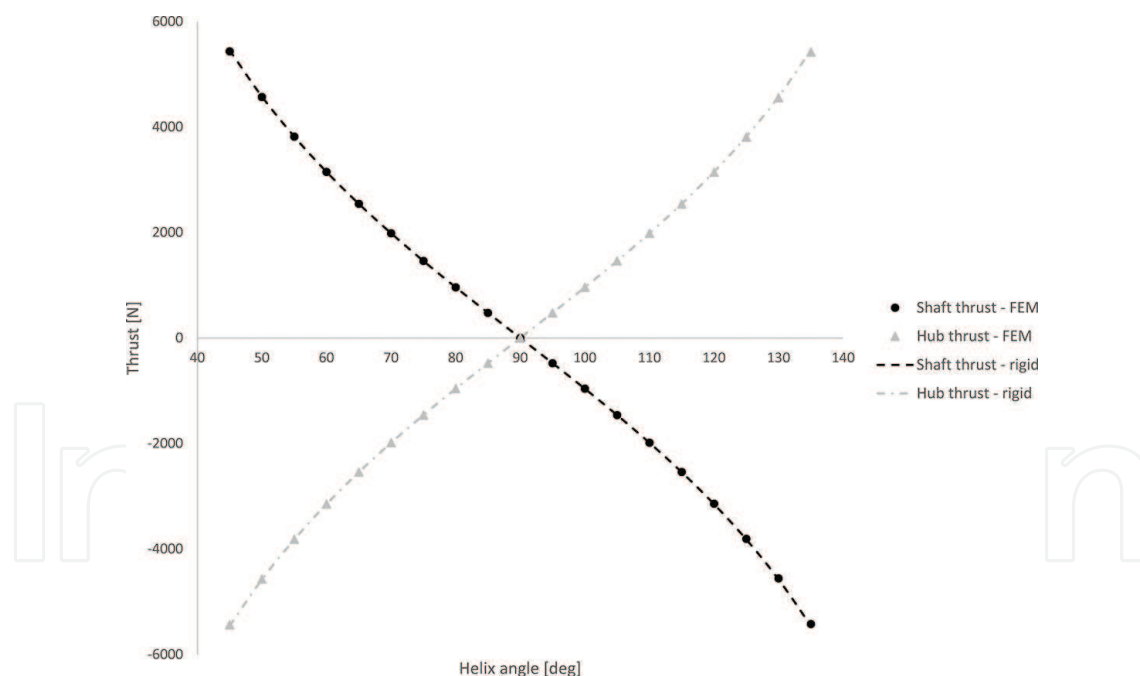

Figure 10. Reactions of shaft and hub constraints for different helix angles under torque load.

4.5. Design of the support system

In the following, the above-explained laws of load distribution are used to choose the design parameters in the assumption, adopted for the sake of simplicity, that the members of the spline pair are stiff. Such an assumption does not lead to significant errors, as proved above.

By means of the resulting design procedure, the load distribution in nominal operating conditions between the two axial bearings can be set by means of a proper choice of the helical angle. To this purpose, **Figure 11** shows for the data reported in **Tables 1** and **2** (Case B) the load transfer through the coupling together with the corresponding axial loads of the bearings as a function of the helix angle β in nominal working conditions.
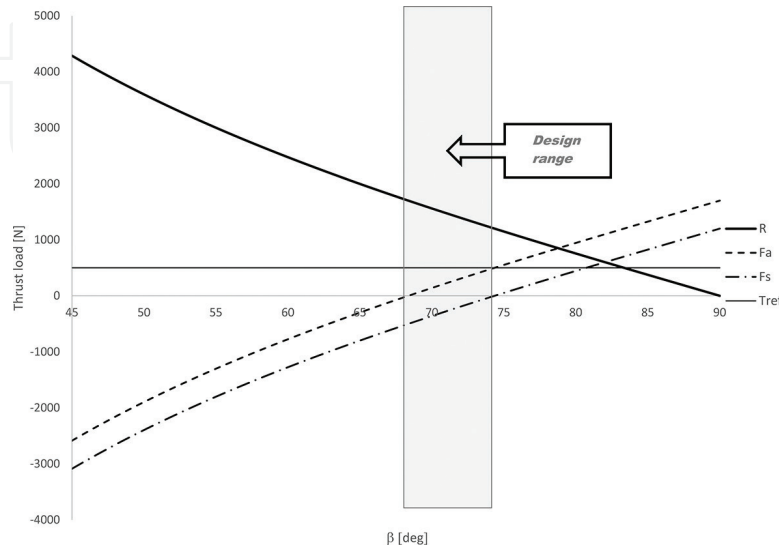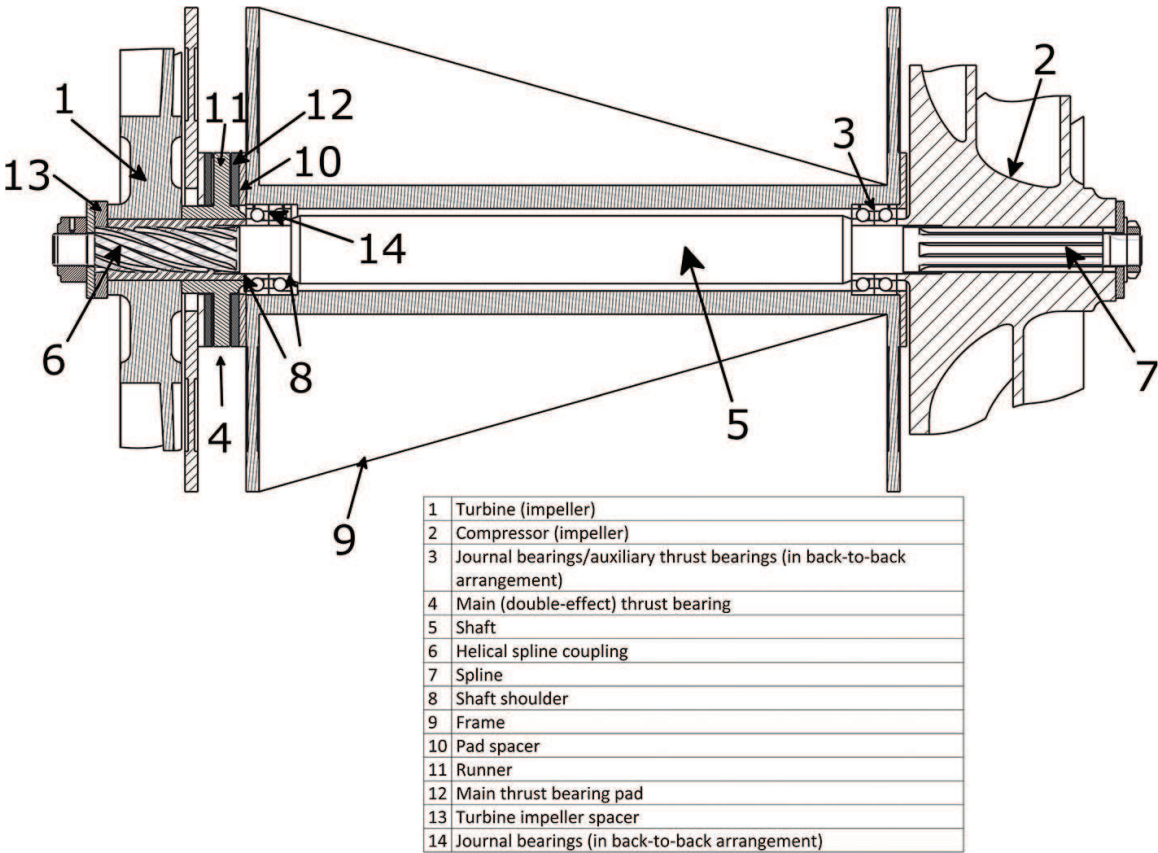

Figure 11. Trends of axial bearing thrusts and load transfer as a function of helix angle in nominal operating conditions.

By assuming that positive torque acts on a turbine impeller ($M = M_t > 0$), handedness of the helix must be chosen so that the load transfer R is directed as in **Figure 7**. In other words, the spline coupling must exert (equal) axial forces R opposite to F_t and F_c on the hub and the shaft, respectively. According to Eq. (1), such a condition yields that the range of helix angle in the abscissa of the plot in **Figure 11** cannot exceed 90°.

The load transfer R (thick solid curve) is plotted in **Figure 11** according to Eq. (1). On the basis of its trend, the axial thrusts F_a and F_s that turbine and shaft, respectively, exert on the main bearing (4) and on the auxiliary bearing (3) are plotted as dashed and dash-dotted curves. They are evaluated by means of the relations $F_a = F_t - R$ and $F_s = F_c - R$, which can be deduced by the analysis of **Figure 7**, where turbine and compressor thrusts F_t and F_c are obviously constant in nominal operating conditions. The gray solid horizontal line represents the value of the reference load $T_{ref} = F_t - F_c$, which has to be carried by the single thrust bearing of a conventional machine. As reported in the paragraph dealing with layout and clearly visible in **Figure 11**, when a straight grooved spline ($\beta = 90°$) is picked, the load acting on the main axial bearing (4) is greater than in a conventional plant. Indeed, it is equal to the total turbine thrust F_t, while the auxiliary axial bearing (3) supports the compressor thrust F_c. By reducing the helix angle, the loads acting on both bearings begin to decrease, since the helix is oriented in such a way as to exert on the shaft and the turbine impeller a thrust R opposite to F_c and F_t, respectively (**Figure 7**). Particularly, by choosing β roughly equal to 74°, the main axial bearing (4) must carry the reference load ($F_a = T_{ref}$), while the auxiliary one is axially unloaded and, therefore, since it is only subjected to the (light) radial load, it will have an average life exceeding 6 million hours, as specified in the first row of **Table 5**. Differently, for design values of β ranging between 68 and 74°, the load of the main bearing (4) becomes lower than the

reference one, at the expense of the duration of the auxiliary bearing (3), on which the shaft exerts a negative thrust F_s (directed from the turbine to the compressor). For $\beta = 68°$ the load on the main axial bearing (4) is null and, consequently, the thrust exerted by the shaft on the auxiliary bearing (3) assumes its maximum value, i.e., $F_s = -T_{ref}$. In such a condition, the rolling element bearing (3) exhibits the same duration as in a conventional layout (e.g., see the basic rating life reported in the last two rows of **Table 5**). Obviously, since in the simplified layout of **Figure 4**, the main foil bearing is not of double effect, helix angles lower than 68°, which moreover would lead to an even more unsuitable life of the auxiliary bearing, are forbidden. A good design may require a helix angle slightly reduced in comparison with a value of 74°, where the amount of such reduction can be evaluated by taking into account the life and the reliability required for the bearing (3). In the design range, the highest life/reliability of auxiliary bearing (3) is obtained for $\beta = 74°$, while the lowest one, typical of a conventional layout, for $\beta = 68°$; the most severe loading case for the main axial bearing (4), equivalent to that of a conventional layout, occurs at $\beta = 74°$, the most favorable one (zero thrust) at $\beta = 68°$.

Finally, the actual assembly drawing of the invention, suited to both Cases A and B of **Table 2** as well as transient loading conditions, is reported in **Figure 12**. In this case, the total hot clearance between runner (11) and pads (12) of the double-effect air bearing must be higher than that between turbine impeller (1) and the spacer (13) used to adjust the impeller axial clearance. The second set of (nonlocating) angular contact bearings (14) cited in paragraph 4.1 is added.

1	Turbine (impeller)
2	Compressor (impeller)
3	Journal bearings/auxiliary thrust bearings (in back-to-back arrangement)
4	Main (double-effect) thrust bearing
5	Shaft
6	Helical spline coupling
7	Spline
8	Shaft shoulder
9	Frame
10	Pad spacer
11	Runner
12	Main thrust bearing pad
13	Turbine impeller spacer
14	Journal bearings (in back-to-back arrangement)

Figure 12. Section of the micro-GT support system assembly designed according to the invention.

5. Conclusions

For adoption in microturbines, the only conventional rolling element supports selected from manufacturers' catalogs (without including ad hoc solutions) compatible with the speeds at the hand are high-precision angular contact ball bearings, preferably with ceramic parts. Particularly, hybrid bearings allow for a perceivable increase in maximum speed, while all ceramic bearings can reach the high operative temperatures suitable for micro-GT units.

Air supports (hybrid aerostatic as well as aerodynamic) are the most suited oil-free solution for this application. They offer the best compromise between installation costs and performance for micro-GT systems. Aerodynamic bearings are preferred since they need no external supply of pressurized gas (e.g., tapped from the compressor) as they are self-acting. Particularly, foil bearings have good stability and compensate for shaft thermal expansion. Their main drawback is the short phase of dry friction during start up and stop, which limits their life.

Magnetic bearings are another promising oil-free solution. PMBs are suitable for speed and ease of miniaturization as well as independence from external energy input, but the high temperature limits the use of permanent magnets in microturbines since these could demagnetize. Consequently, electromagnets must be employed, although they consume a considerable amount of electrical energy. AMB remains the most suitable magnetic-driven solution because of high speed, temperature, and the control of machine dynamics.

The comprehensive comparison among the different reliable technologies carried out in the first part of this chapter proves that the design of an optimal support system might employ different type of bearings. Indeed, each of them have peculiar capabilities and limits, which make them suitable for particular tasks, e.g., carrying high load continuously or low load during frequent start/stops, working at high or low temperature, etc.

An innovative support system that relies on air as well as rolling element bearings and employs spline couplings has been proposed. The particular bearing arrangement devised for the new system is capable of taking advantage of the best characteristics of both bearing types and, simultaneously, of minimizing the effects of their flaws. Particularly, rolling element bearings behave much better than air bearings during start-stops but ensure limited duration under nominal load and speed of the most efficient micro-GT units. On the contrary, (air) foil bearings provide suitable life and load-carrying capabilities in nominal working conditions but cannot withstand a large number of start-stop cycles of the units. Therefore, the proposed system is designed to switch between the two types of bearings automatically when the unit ends the transient operation. In addition, it employs helical splines as both convenient coupling systems and actuators for the load partition between the two bearing types. Indeed, partitioning the turbine thrust is required in order to optimize the behavior of the support system.

The invention performs better than conventional support systems based on rolling element bearings, since it radically increases bearing life or load-carrying capacity as well as working temperature. In comparison with modern systems based on foil bearings, the invention is advantageous in that the number of start-stop cycles of the machine is not limited, solid

lubrication is not required, the power of the starter can be reduced and retrofitting conventional machines based on rolling element bearings is possible. In any case, replacing shrink fittings with spline couplings can simplify maintenance and inspection of the impellers. Although the proposed support system is not oil-free, the concepts used in its development might be adopted in order to match other type of bearings. For instance, combining thrust foil bearings and radial magnetic bearings may yield an oil-free design with still higher performance.

Author details

Fabrizio Stefani*, Andrea Perrone, Luca Ratto and Ramon Francesconi

*Address all correspondence to: stefani@unige.it

Department of Mechanical, Energy, Management, and Transportation Engineering, University of Genoa, Genoa, Italy

References

[1] do Nascimento M.A.R., de Oliveira Rodrigues L., dos Santos E.C., Gomes E.E.B., Dias F.L.G., Velásques E.I.G., Carrillo R.A.M. Micro Gas Turbine Engine: A Review. In: Benini E., editor. Progress in Gas Turbine Performance. Rijeka, Croatia: InTechOpen; 2013. p. 107–141. DOI: 10.5772/54444.

[2] Section 5. Technology Characterization-Microturbines. In: Catalog of CHP Technologies. U.S.: EPA & CHP; 2014.

[3] Hamilton S.L. The Handbook of Microturbine Generators. Tulsa, Oklahoma: PennWell; 2003. 205 p.

[4] Barsi D., Garbarino T., Perrone A., Ratto L., Ricci G., Stefani F., Zunino P. Micro Gas Turbine Integrated Design: Thermodynamic Cycle, Combustor, Recuperator and Bearings (Part 1). In: Fourth International Conference of Energy Water and Environmental Sciences; 15–17 December 2015; Ras Al Khaimah, United Arab Emirates.

[5] Isomura K., Togo S.I., Tanaka S. Study of Micro-High Speed Bearings and Rotor Dynamics for Micromachine Gas Turbines, Paper 7. In: Micro Gas Turbines. Educational Notes RTO-EN-AVT-131. France: Neuilly-sur-Seine; 2005.

[6] Signer H., Bamberger E.N., Zaretsky E.V. Parametric Study of the Lubrication of Thrust Loaded 120-mm Bore Ball Bearings to 3 Million DN. Journal of Lubrication Technology. 1974;**96**:515–526.

[7] Zwyssig C., Member S., Kolar J.W., Member S., Round S.D. Megaspeed Drive Systems : Pushing Beyond 1 Million r/min. IEEE/Asme Transactions on Mechatronics. 2009;**14**:564–574.

[8]   Akamatsu Y., Mori M. Development of Eco-Friendly Oil Jet Lubricated. NTN Technical Review. 2004;**72**:6–10.

[9]   Popp M., Sternagel R. Hybrid Ceramic and All Ceramic Anti Friction Bearings. European Space Agency-Publications-ESA SP. 1999;**438**:105–110.

[10] Khonsari M.M., Booser E.R. An Engineering Guide for Bearing Selection. Tribology and Lubrication Technology. 2004;**60**:26–32.

[11] Finley W.R., Hodowanec M.M. Sleeve versus Antifriction Bearings: Selection of the Optimal Bearing for Induction Motors. IEEE Transactions on Industry Applications. 2002;**38**:909–920.

[12] Waumans T., Peirs J., Al-Bender F., Reynaerts D. Design, Optimisation and Testing of a High-Speed Aerodynamic Journal Bearing with a Flexible, Damped Support. In: Tech Dig PowerMEMS 2009; 1–4 December 2009; Washington, DC, USA. 2009. p. 83–86.

[13] Waumans T., Peirs J., Al-Bender F., Reynaerts D. Aerodynamic Journal Bearing with a Flexible, Damped Support Operating at 7.2 Million DN. Micromechanics Microengineering. 2011;**21**:104014.

[14] Hikichi K., Isomura K., Saji N., Esashi M., Tanaka S. Ultra-High-Speed Tape-Type Radial Foil Bearing for Micro Turbomachinery. In: Proc. PowerMEMS 2009; 1–4 December 2009; Washington, DC, USA. 2009.

[15] Schiffmann J. Enhanced Groove Geometry for Herringbone Grooved Journal Bearings. Journal of Engineering Gas Turbines Power. 2013;**135**:102501.

[16] Stanev P.T., Wardle F., Corbett J. Investigation of Grooved Hybrid Air Bearing Performance. Proceedings of the Institution of Mechanical Engineers, Part K: Journal of Multi-body Dynamics. 2004;**218**:95–106.

[17] Peirs J., Waumans T., Vleugels P., Al-Bender F., Stevens T., Verstraete T., et al. Micropower Generation With Microgasturbines: A Challenge. Proceedings of the Institution of Mechanical Engineers, Part C: Journal of Mechanical Engineering Science. 2007;**221**:489–500.

[18] Waumans T., Peirs J., Reynaerts D., Al-Bender F. On The Dynamic Stability of High-Speed Gas Bearings: Stability Study and Experimental Validation. Sustainable Construction and Design. 2011;**2**:1–10.

[19] Görne J. Using Active Magnetic Bearings for High Speed Machining—Conditions and Benefits. In: TEHNOMUS XVII; May 2013; Suceava, Romania. 2013. p. 13–20.

[20] Schweitzer G. Active Magnetic Bearings-Chances and Limitations. In: 6th International Conference on Rotor Dynamics. Australia: Elsevier Ltd.; 2002.

[21] Clark D.J., Jansen M.J., Montague G.T. An Overview of Magnetic Bearing Technology for Gas Turbine Engines. National Aeronautics and Space Administration Technical Memorandum. 2004;NASA/TM-2004-213177:1–13. Available from: https://ntrs.nasa.gov/archive/nasa/casi.ntrs.nasa.gov/20040110826.pdf [Accessed: 2017-01-10].

[22] Cappellino C.A., Osborne J.C. The Prediction of Bearing Lubricant Temperatures and Cooling Requirements for a Centrifugal Pump. In: Proceedings of the Second International Pump Symposium; April 1985; Houston, Texas. 1985. p. 77–84.

[23] Ghosh M., Majumdar B., Sarangi M. Theory of Lubrication. New Delhi: Tata McGraw-Hill; 2013.

[24] DellaCorte C., Lukaszewicz V., Valco M.J., Radil K.C., Heshmat H. Performance and Durability of High Temperature Foil Air Bearings for Oil-Free Turbomachinery. Tribology Transactions. 2000;**43**:774–780.

[25] Venkatesh V. Precision Engineering. New Delhi: Tata McGraw-Hill Education; 2007.

[26] Hamrock B.J., Anderson W.J. Rolling-Element Bearings. National Aeronautics and Space Administration Reference Publication. 1983;NASA RP-1105:1–57. Available from: https://ntrs.nasa.gov/archive/nasa/casi.ntrs.nasa.gov/19830018943.pdf [Accessed: 2017-01-10].

[27] Pope J.E. Rules of Thumb for Mechanical Engineers. Houston, Texas: Gulf Publishing Company; 1997.

[28] Tanimoto K., Ikeda T. Evaluation of Extra-Small Ceramic Ball Bearings. KOYO Engineering Journal English Edition. 2000;**156**(E):23–29.

[29] Powell J. Design of Aerostatic Bearings. Brighton, U.K.: The Machinery Publishing Co.; 1970.

[30] DellaCorte C., Valco M.J. Load Capacity Estimation of Foil Air Journal Bearings for Oil-Free Turbomachinery Applications. STLE Tribology Transactions. 2000;**43**(4):795–801.

[31] Radil K.C., DellaCorte C. Foil Bearing Starting Considerations and Requirements for Rotorcraft Engine Applications. Army Research Laboratory Final Report. 2009;ARL-TR-4873:1–12. Available from: https://ntrs.nasa.gov/archive/nasa/casi.ntrs.nasa.gov/20120012857.pdf [Accessed: 2017-01-10]

[32] DellaCorte C., Radil K. A Preliminary Foil Gas Bearing Performance Map. National Aeronautics and Space Administration Technical Memorandum. 2006;NASA/TM-2006-214343:1–15. Available from: https://ntrs.nasa.gov/archive/nasa/casi.ntrs.nasa.gov/20060051824.pdf [Accessed: 2017-01-10]

[33] Cunningham R.E., Fleming D.P., Anderson W.J. Experiments of Stability of Herringbone-Grooved Gas Lubricated Journal Bearings to High Compressibility Numbers. National Aeronautics and Space Administration Technical Report. 1968;NASA TN-D-4440:1–20. Available from: https://ntrs.nasa.gov/archive/nasa/casi.ntrs.nasa.gov/19680012496.pdf [Accessed: 2017-01-10]

[34] Reitsma T.W. Lifting Off Friction [Internet]. 1 September 2006. Available from: http://machinedesign.com/archive/lifting-friction.

[35] Montague G., Jansen M., Provenza A., Jansen R., Ebihara B., Palazzolo A. Room Temperature Characterization of a Magnetic Bearing for Turbomachinery. National Aeronautics and Space Administration Technical Memorandum. 2002;NASA/TM–2002-211904:1–9.

Available from: https://ntrs.nasa.gov/archive/nasa/casi.ntrs.nasa.gov/20020090900.pdf [Accessed: 2017-01-10]

[36] Montague G., Jansen M., Provenza A., Palazzolo A., Jansen R., Ebihara B. Experimental High Temperature Characterization of a Magnetic Bearing for Turbomachinery. National Aeronautics and Space Administration Technical Memorandum. 2003;NASA/TM–2003-212183:1–12. Available from: https://ntrs.nasa.gov/archive/nasa/casi.ntrs.nasa.gov/20030039177.pdf [Accessed: 2017-01-10]

[37] Paden B., Groom N., Antaki J.F. Design Formulas for Permanent-Magnet Bearings. ASME Journal of Mechanical Design. 2003;**125**:734–738.